International Journal of Concrete Structures and Materials

RESEARCH Open Access

Shear Strengthening of RC Beams Using Partial-Length Near-Surface Mounted (PLNSM) CFRP Strips

Senghong Khol[1], Soo-Yeon Seo[1*], Hai Van Tran[1] and Muhammad Usman Hanif[1,2]

Abstract

Shear strengthening of reinforced concrete beams using near-surface mounting (NSM) method with fiber-reinforced polymer (FRP) strips is more effective because of improved bond strength, better fire resistance and high maintainability. However, the surface preparation for NSM method is a difficult process where the beam–slab corner is not accessible by the rotary blade of the groove-making equipment. Consequently, the application of NSM method becomes more difficult to apply. Therefore, in this study, the effect of reducing in NSM length on the shear strength has been investigated by reinforcing only a part of the height, not the entire web of beam, referred to as the partial-length NSM method (PLNSM). Half scaled five RC T-beams were made and tested under symmetrical four-point static loading system. All except one was strengthened in shear in which the effect of reduced NSM length was balanced by inclining the partial-length NSM strips (IPLNSM). Furthermore, to mitigate the detrimental effect of reduced lengths of NSM strips, the retrofitting was enhanced by additional externally bonded reinforcement (EBR) method using CFRP sheets. The results showed that there was no significant negative effect of reduced NSM length on the strength of the strengthened specimens, and by providing inclined NSM strips, significant improvement in the strength was observed. Additionally, the hybrid approach combining the inclined partial length NSM (IPLNSM) and EBR method showed improvement in strength and deflection capacity. Lastly, when compared with the currently available design procedures, it was found that the available formulation can predict the design strength of PLNSM and IPLNSM reinforcement, thus making them a viable option for retrofitting reinforced concrete beams.

Keywords Shear strengthening, Near-surface-mounted (NSM), Partial length NSM (PLNSM), T-beams, Hybrid approach, RC beams

1 Introduction

Reinforced concrete (RC) structures are constantly exposed to unprecedented harsh environments which degrade these structures over time. Additionally, with the more research and development, the serviceability requirements of the structures have become more stringent. Consequently, the structures are retrofitted using fiber-reinforced polymer (FRP) reinforcement to meet the additional strength and serviceability requirements. Generally, three types of materials are used for retrofitting, such as carbon, aramid and glass. Two commonly used methods in structural strengthening are by using externally bonded reinforcement (EBR) and near-surface-mounting (NSM) methods. The former involves laying the FRP sheet on the concrete surface using epoxy resin and the latter involves making grooves or slits on the concrete surface and embedding

Journal information: ISSN 1976-0485 / eISSN 2234-1315.

*Correspondence:
Soo-Yeon Seo
syseo@ut.ac.kr
[1] Department of Architectural Engineering, Korea National University of Transportation (KNUT), 27389 Chungju, South Korea
[2] Department of Technology and Innovation, SDU Civil and Architectural Engineering, University of Southern Denmark, Campusvej 55, 5230 Odense, Denmark

Springer Open

© The Author(s) 2024. **Open Access** This article is licensed under a Creative Commons Attribution 4.0 International License, which permits use, sharing, adaptation, distribution and reproduction in any medium or format, as long as you give appropriate credit to the original author(s) and the source, provide a link to the Creative Commons licence, and indicate if changes were made. The images or other third party material in this article are included in the article's Creative Commons licence, unless indicated otherwise in a credit line to the material. If material is not included in the article's Creative Commons licence and your intended use is not permitted by statutory regulation or exceeds the permitted use, you will need to obtain permission directly from the copyright holder. To view a copy of this licence, visit http://creativecommons.org/licenses/by/4.0/.

the FRP materials inside the grooves. EBR method has shown strength improvement in flexure as well as shear (Al-Amery & Al-Mahaidi, 2006). In shear retrofit, anchoring the FRP material substantially increases the shear strength but at the cost of using intrusive methods (Arslan et al., 2022; Bae & Belarbi, 2013; Barris et al., 2018; Dias et al., 2021, 2021; El-Maaddawy & Chekfeh, 2012; Godat et al., 2020; Mhanna et al., 2021; Moradi et al., 2020; Oller et al., 2019; Tanarslan et al., 2021). NSM method, on the other hand, is more effective in terms of application. It has been shown experimentally that the NSM method utilizes the complete strength of the FRP material. In addition, the NSM strengthening method provides higher durability since the FRP material is embedded in concrete and epoxy which protects it from external effects while preserving the original physical appearance of the structure (Hassan & Rizkalla, 2004; Hong et al., 2011; Seo et al., 2013, 2016a, 2016b; Sharaky et al., 2014).

Considering the advantages of NSM method, shear strengthening using this method has been extensively researched in the past. It has been found that NSM retrofitting offers greater shear strengthen compared to the EBR method (Al Rjoub et al., 2019; Barros & Dias, 2006; Dias & Barros, 2010, 2013, 2017; Jalali et al., 2012; Lorenzis & Nanni, 2001; Mostofinejad et al., 2019; Nanni et al., 2004; Rizzo & De Lorenzis, 2009). Fig. 1 compares three shear strength improvements using vertical EB FRP (EBR-V), 45-degree NSM FRP (NSM-45), and vertical NSM FRP (NSM-V). It can be seen that the vertical NSM method increases the strength substantially more than the EBR method and further increases the strength when they are inclined at an angle. However, the groove preparation is generally carried out using a rotary blade which cannot access the beam–slab corner, indicated as an inaccessible region in Fig. 2. From a practical point of view,

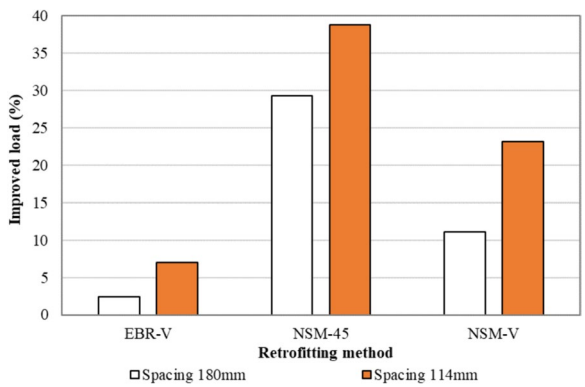

Fig. 1 Strength improvement corresponding to shear strengthening method (Dias & Barros, 2010)

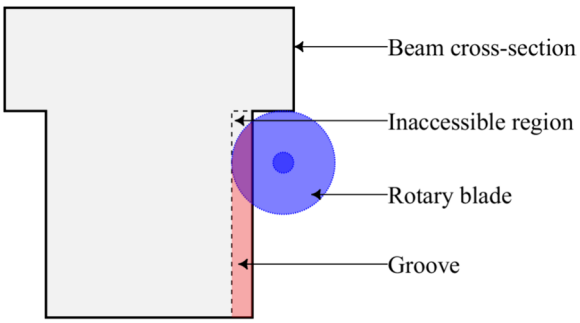

#. 2 Preparation of grooves for shear retrofit using NSM method

making groove in this region complicates the retrofitting process.

As one way, it is possible to consider partial length NSM FRPs in the shear strengthening. Regarding the study for partial length FRP, Al Rjoub et al. (2019) conducted a test and revealed that the shear strength of RC beams using PLNSM was found to be inversely proportional to length reduction. And reducing the CFRP lengths affected the failure mode due to cracks spreading outside the retrofitted area. Therefore, the cracks were not completely intercepted by NSM FRP in case of short partial length. It means that the way to intercept cracks by FRP need to be developed when the PLNSM is applied for shear strengthening. So, it can be said that more studies are necessary to obtain useful results for finding an effective way in the application of partial length NSM FRP for shear strengthening.

Therefore, this research experimentally investigated the performance of shear retrofit using partial-length NSM strips and inclined partial-length NSM strips, referred to as PLNSM and IPLNSM hereafter, respectively. Furthermore, to mitigate the detrimental effect of reduced lengths of NSM strips, the retrofitting was enhanced by additional EBR retrofit using CFRP sheets. Finally, the strength of PLNSM was estimated using the available design formulations.

2 Experimental Investigation

2.1 Test Specimens

To achieve the research objectives, five T-shaped RC beams with identical geometric and material properties were fabricated in accordance with ACI 318-19 (2019). Each specimen was planned to be half-scale and reinforced with four D13 and three D13 rebars for tension and compression, respectively. Shear reinforcement was provided using D10 rebar at 130-mm spacing. All specimens were retrofitted for flexure using the partially debonded NSM method (Seo et al., 2016a, 2016b) to increase the flexural capacity of the specimens and

evaluate the effect of shear cracks occurred at the anchorage zone on the flexural strength. Shear strengthening was carried out on the specimens using PLNSM, IPLNSM and hybrid IPLNSM-EBR methods, as summarized in Table 1.

The material properties of concrete, rebar and FRP can be found in Table 2.The CFRP strip used for flexural reinforcement was a carbon fiber-based strip with a thickness of 3.6 mm and a width of 15 mm, with a total length of 1600 mm. After forming a groove on the surface of the specimen with a depth of 17 mm and a width of 8 mm to place the CFRP strip, epoxy mortar (SIKADUR 31) was filled with 500 mm at both ends to bond the CFRP strip, and the central part of 600 mm was left in a non-adhesive state. Additionally, the material properties of the retrofitting materials are summarized in Table 3. The geometric, reinforcement and flexural retrofit details are depicted in Fig. 3.

2.2 Shear Strengthening

For shear strengthening, CFRP strips measuring 1.2 mm in thickness and 15 mm in width were employed as NSM shear reinforcement. The reduction in NSM length, kept at 60% of the web height as 120 mm, was the primary variable in this research. This value was chosen regarding practical application using a rotary blade and to ensure the quality of the groove at the bottom of slab. Additional variables considered in this research included using IPLNSM and combining the IPLNSM with EBR method using U-wrap CFRP sheets.

Fig. 4 presents strengthening detail for all specimens. The specimen TC serves as the reference beam without

Table 1 List of specimens

Specimen name	Flexural retrofit method and quantity	Shear retrofit				
		Retrofit method	Quantity	Height of embedded NSM strip (mm, %)	Angle	Space (mm)
TC	Partially debonded NSM method, Strip (3.6 × 15 mm^2)	None	–	–	–	–
TP-3I90		PLNSM	3 strips (1.2 × 15 mm^2)	120, 60	90°	150
TP-3I45		IPLNSM	3 strips (1.2 × 15 mm^2)	120, 60	45°	150
T2L		EBR	2 layers of CFRP sheet (0.111 × 300 mm^2)	200, 100	–	–
TP-2I45-2L		IPLNSM	2 strips (1.2 × 15 mm^2)	120, 60	45°	180
		EBR	2 layers of CFRP sheet (0.111 × 300 mm^2)	200, 100	–	–

Table 2 Material properties of the RC beam and retrofit materials

Material		Yield strength (MPa)	Compressive strength (MPa)	Tensile strength (MPa)	Young's modulus (GPa)	Maximum strain (%)
Concrete		–	26	–	–	0.3
Rebar diameter	D10	467.4	–	612.8	200.0	–
	D13	547.9	–	652.0	200.0	–
CFRP strip	1.2 mm	–	–	1794	167.0	1.07
	3.6 mm	–	–	2175	162.9	1.31
CFRP sheet	0.111 mm	–	–	2395	148.14	1.61

Table 3 Material properties of epoxies given by the manufacturer

Epoxy type	Tensile strength (MPa)	Compressive strength (MPa)	Modulus of elasticity (MPa)
Epoxy for CFRP strip (SIKADUR 31)	20	103	5,485
Epoxy for CFRP sheet (SIKADUR 330K—primer)	49	78	–
Epoxy for CFRP sheet (SIKADUR 330K—resin)	59	108	–

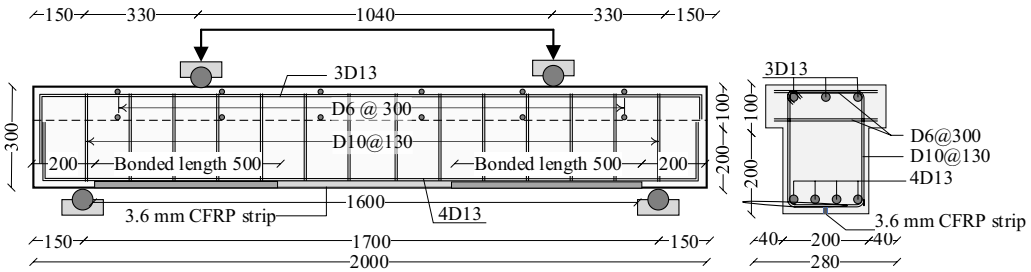

Fig. 3 Geometric and reinforcement details of the beam specimens (unit: mm)

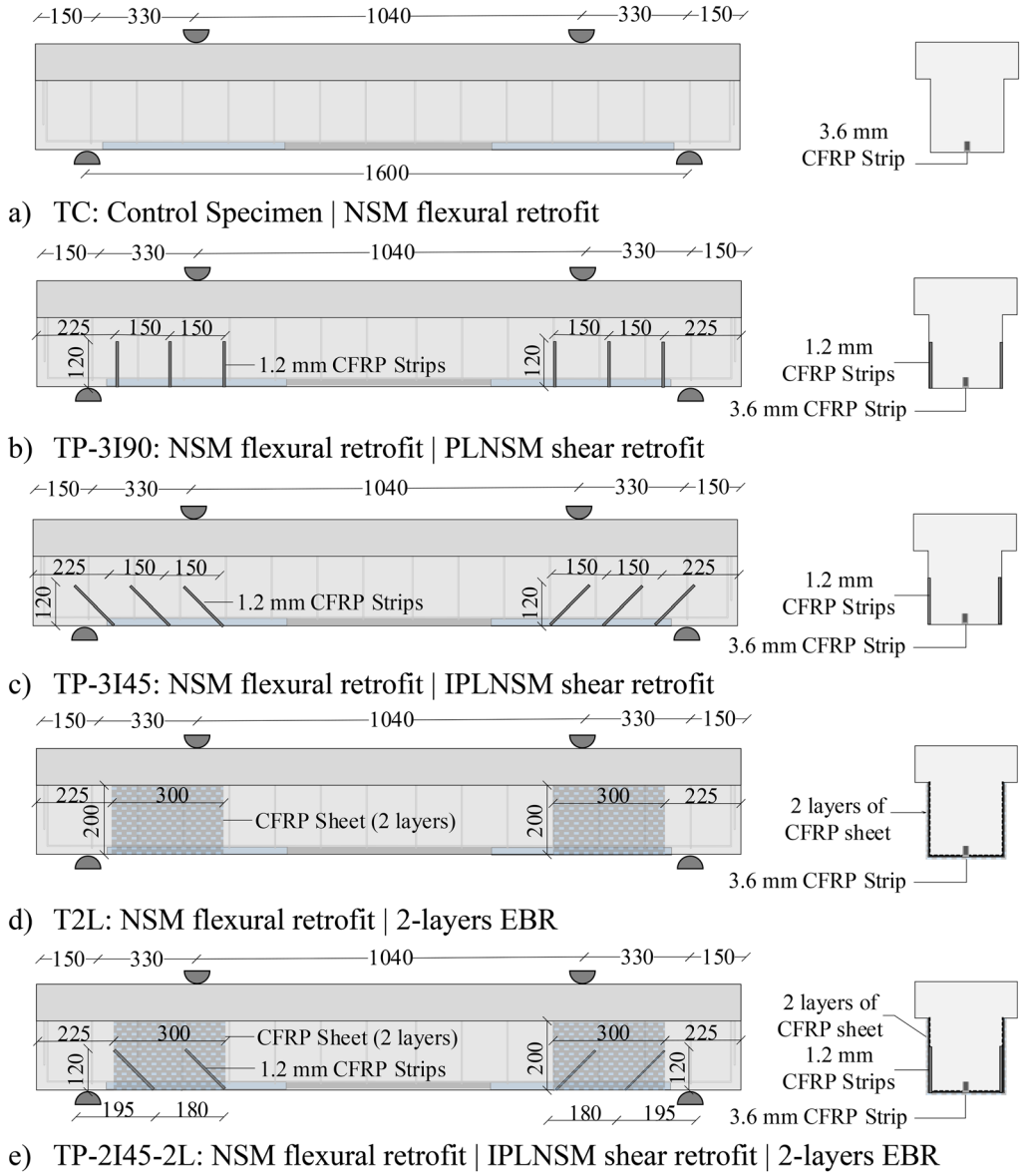

Fig. 4 Details of the shear-strengthened specimens (unit: mm)

any shear strengthening as shown in Fig. 4a. The Specimens TP-3I90 and TP-3I45 were strengthened using NSM CFRP strips with a spacing of 150 mm and inclinations of 90° and 45°, respectively (Fig. 4b, c). T2L specimen was only strengthened using EBR U-wrap CFRP-sheet (Fig. 4d), while the TP-2I45-2L specimens were strengthened initially by NSM CFRP strip with a spacing of 180 mm and inclined angles of 45°, and then the U-wrap CFRP sheet was applied over it using EBR method with epoxy (SIKADUR 330K); a CFRP sheet with a thickness of 0.111 mm and a width of 300 mm was used for the EBR retrofit as shown in Fig. 4e.

The retrofit process for the NSM method involved placing the CFRP strips in grooves made on the web, with a width and depth of 5 and 17 mm, respectively. Epoxy mortar was prepared according to the manufacturer's recommended procedures. The grooves were filled with epoxy (SIKADUR 31) and then the CFRP strips were inserted into these grooves. The details of these steps are illustrated in Fig. 5a–d. The retrofitting step of EBR method is illustrated in Fig. 5e–g. The final retrofitted specimen can be seen in Fig. 5h.

2.3 Setup for Test

Four-point load configuration was selected for the test. The shear span-to-depth ratio (a/d) was maintained at 1.25 to ensure the shear mode of failure. All specimens were attached with the strain gauges at the mid-span of the CFRP flexure reinforcement denoted by FS, and strain gauges for CFRP shear reinforcement were attached to all specimens except TC but only activated in TP-3I45 and TP-2I45-2L. Strain gauges on CFPR strip were attached at mid-height of each strip and additional strain gauges on CFRP sheet were attached at the same location as strip for specimen TP-2I45-2L (S on strip and L on sheet), as shown in Fig. 6. Three LVDTs were placed at third points to record the vertical deflection during the test. The testing was carried out using Universal

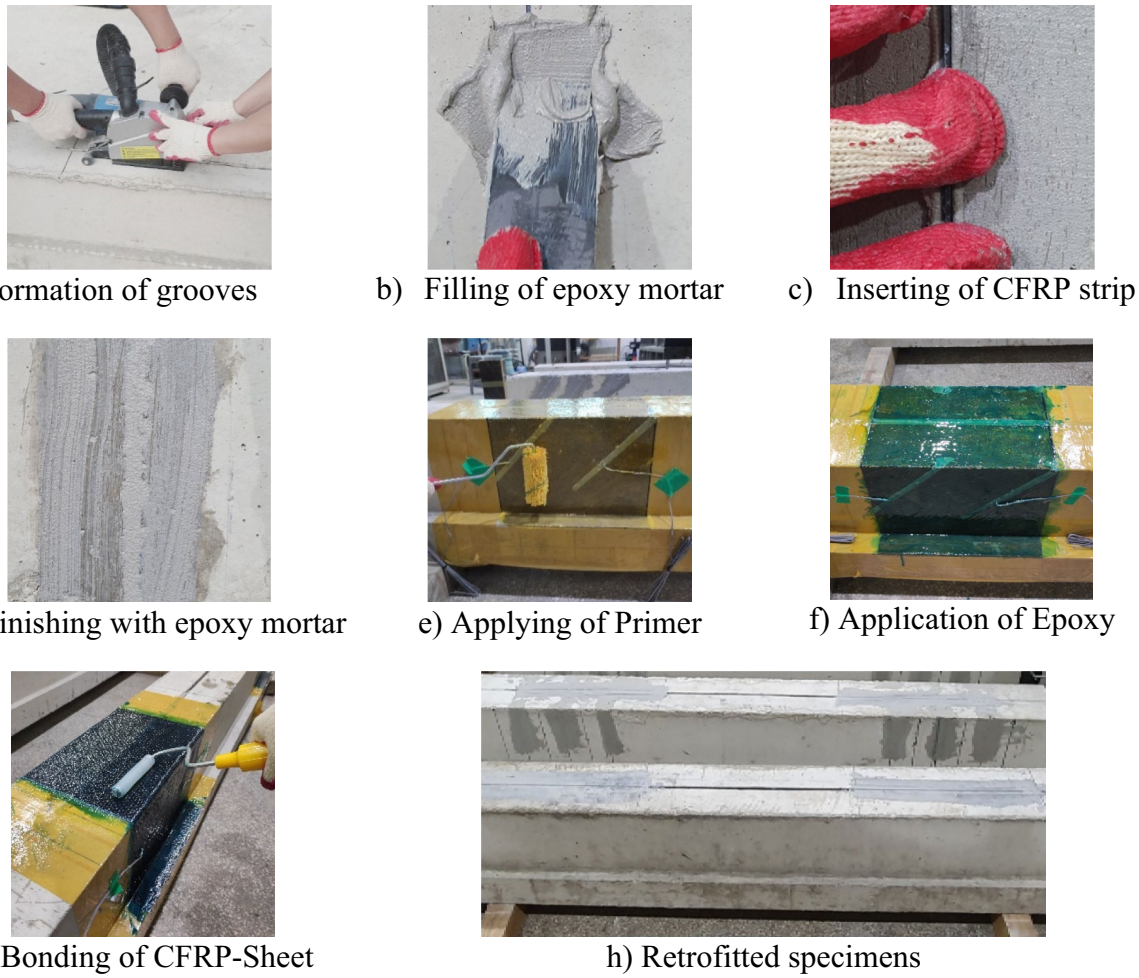

Fig. 5 Strengthening process of specimens

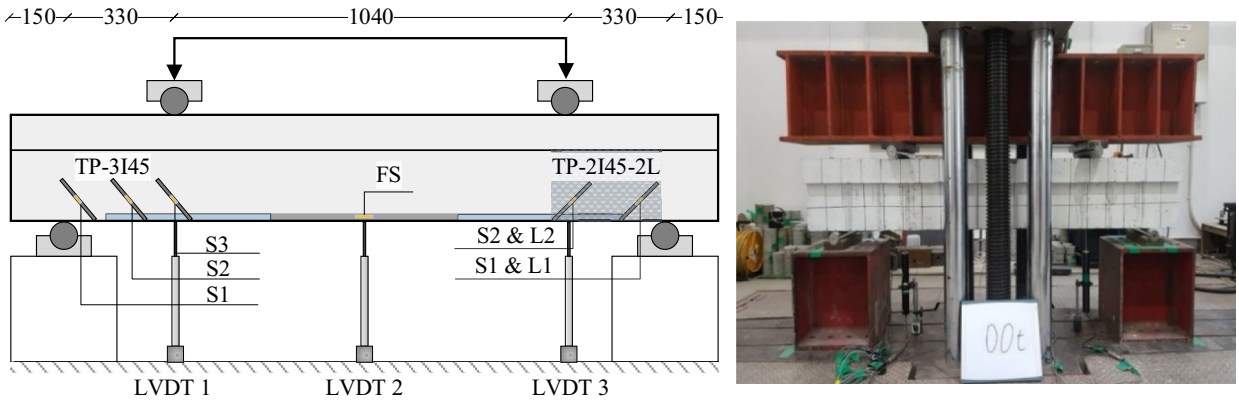

Fig. 6 Test setup

Testing Machine (UTM) with a capacity of 2,000 kN. A displacement-controlled loading was applied with a rate of 0.01 mm/s. During test, cracks were marked on the surface of the specimens until they reached the failure load.

3 Results and Discussion

3.1 Crack and Failure Shapes

The failure modes of all the specimens are depicted in Fig. 7, with more detailed crack patterns within the shear region shown in Fig. 8. Early initiation of flexural cracking was observed in the specimens strengthened with inclined CFRP strips TP-3I45 and TP-2I45-2L. This observation suggests that inclining the strips increased the stiffness of the shear span, leading to early stress concentration in the constant moment region. All beams primarily failed in shear as evidenced by the appearance and opening of diagonal tension cracks. Additionally, an improvement in initial cracking load was observed in all the specimens compared to the TC specimen. Consequently, the presence of shear retrofitting effectively improves the shear performance.

In the TC specimen, a clear diagonal shear crack developed from the support to the loading point, leading to a pure shear failure (Fig. 8a). In contrast, in the TP-3I90 specimen, multiple shear cracks developed, with some of them being intercepted by CFRP strips at lower load levels. As the load increased, several diagonal cracks appeared on the top of web and in the flange region where the CFRP strip was not provided (Fig. 8b). Specifically, the angle of the diagonal shear cracks was steeper compared to that observed in the TC specimen, and multiple cracks developed between CFRP strips. These findings suggest that the PLNSM strips contributed to the pivoting of the shear cracks.

For specimen TP-3I45, the shear crack was intercepted by the second CFRP strip, after which additional cracks developed and propagated towards the top (Fig. 8c).

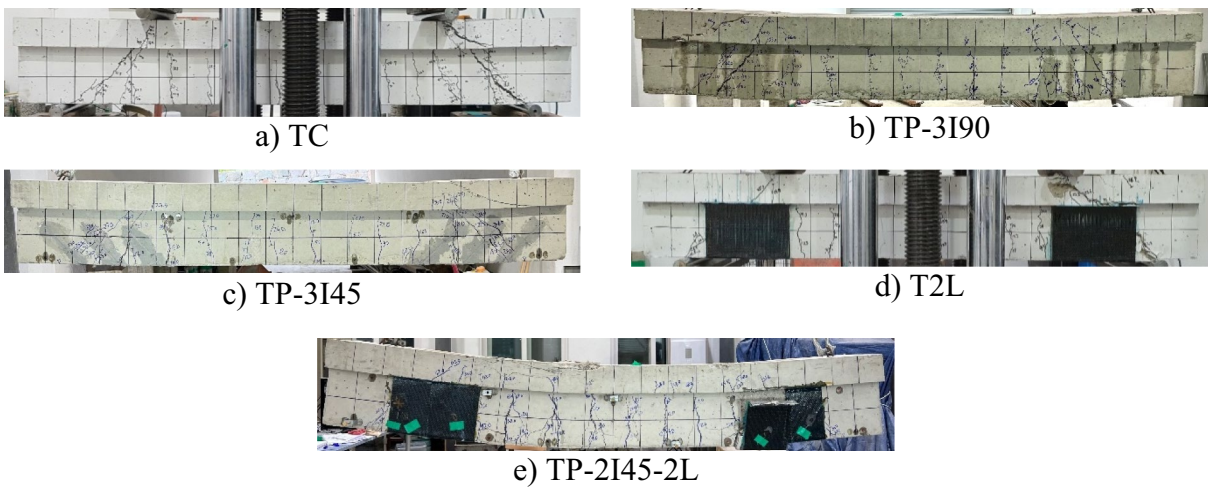

Fig. 7 Failure shapes of the test specimens

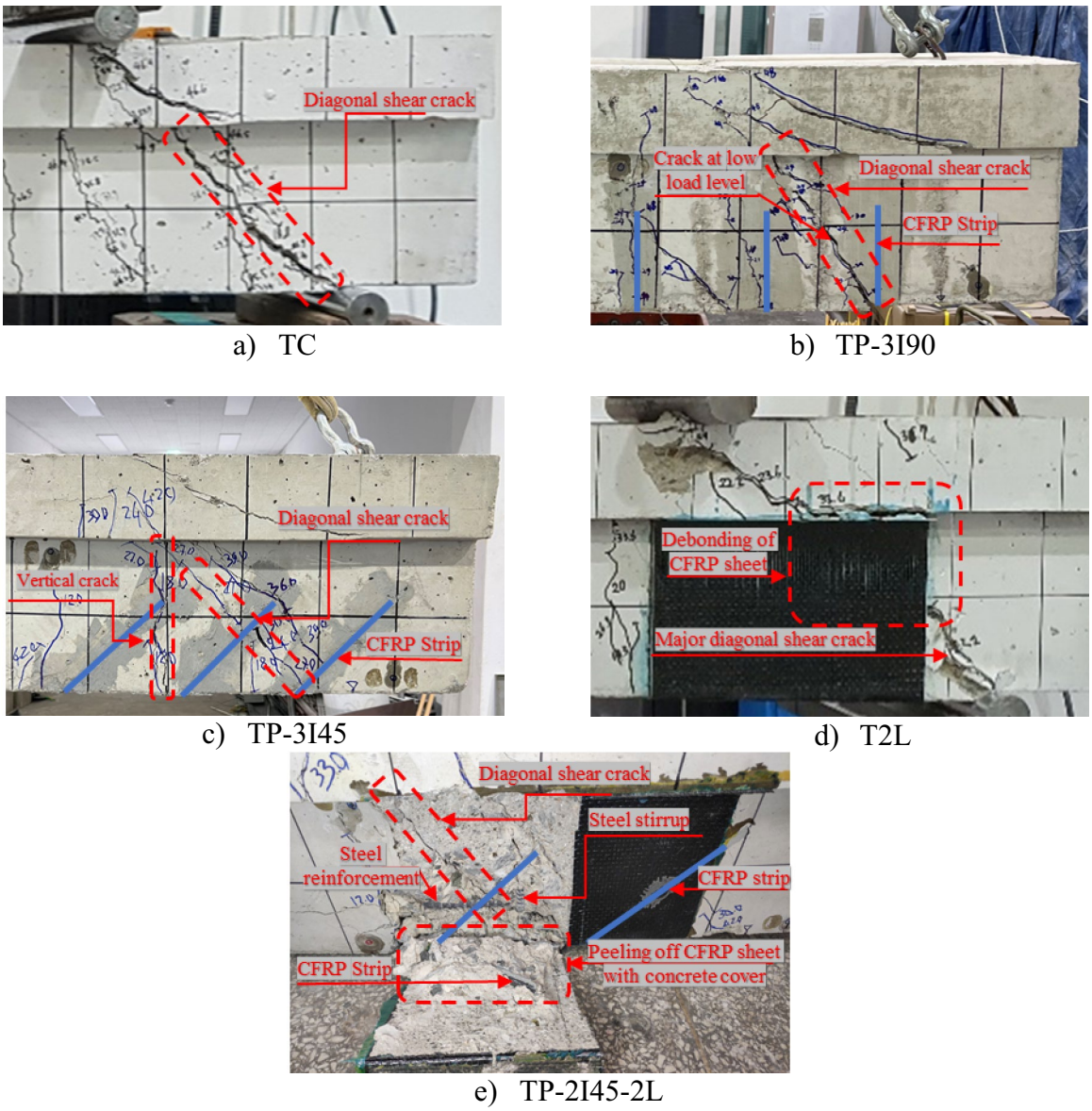

Fig. 8 Detailed crack shapes in the shear region

Subsequently, these cracks were intercepted by the first CFRP strip. However, the vertical cracks also appeared in the shear span. Based on the observed crack formations, it was noted that providing an inclination to CFRP strips improves the retrofit efficiency, despite the reduced length.

In specimens T2L and TP-2I45-2L, initial shear cracks were observed predominantly in regions outside the retrofitted areas due to the presence of CFRP sheets on the beam surface. Notably, in TP-2I45-2L, the initial shear crack developed at a later stage compared to specimen T2L. Subsequently, diagonal tensile cracks developed from the support to the load point, resulting in shear failure (refer to Fig. 8d for T2L specimen). Upon failure, delamination of CFRP sheet was observed with substrate indicating the cohesion failure. Conversely, in TP-2I45-2L specimen, the first layer of the combined IPLNSM CFRP strip and EBR CFRP sheet effectively obstructed the crack propagation while keeping the CFRP sheet intact. Nevertheless, strong peeling-off of the CFRP sheet was observed at the location where the NSM CFRP strip was absent (Fig. 8e), In addition, overall flexural cracking was more pronounced in TP-2I45-2L compared to all other specimens. These observations highlight that the presence

Table 4 Experimental results summary

Specimen name	Initial crack						Ultimate			Failure			ΔP (%)
	Flexural			Shear									
	P_{cf} (kN)	δ_C (mm)	δ_L (mm)	P_{cs} (kN)	δ_C (mm)	δ_L (mm)	P_u (kN)	δ_C (mm)	δ_L (mm)	P_f (kN)	δ_C (mm)	δ_L (mm)	
TC	72.01	1.14	0.99	140.95	2.48	1.98	412.60	7.72	6.15	406.97	7.91	6.59	–
TP-3I90	78.25	1.21	1.08	158.76	2.76	2.17	469.58	19.13	17.04	453.33	19.27	17.28	13.81
TP-3I45	44.10	0.73	0.84	185.23	3.15	3.15	519.59	19.53	16.86	497.23	20.27	17.79	25.93
T2L	76.77	1.52	1.14	264.61	3.92	2.99	467.87	13.21	9.83	462.60	15.37	11.94	13.40
TP-2I45-2L	43.17	0.696	0.765	262.84	4.80	3.58	528.34	19.79	14.6	511.72	27.19	23.3	28.05

P_{cf} and P_{cs} are loads when flexural and shear cracks occurred, respectively, P_u is ultimate load, while P_f is failure load, δ_C is displacement of LVDT 2, δ_L is average value of LVDT 1 and 3, ΔP is improved ultimate load ratio by CFRP reinforcements

of the CFRP strips can confine the component and increase its stiffness, thereby preventing early failure of the CFRP sheet due to crack opening.

3.2 Load–Deflection Behavior

The loads and displacements corresponding to the initial flexural cracks, shear cracks and ultimate load as well as the failure load, are presented in Table 4 and illustrated in Fig. 9. In the shear failure-dominated mechanism of a member shear-reinforced with FRP, after the load reaches the ultimate load, the deformation increases as it is maintained for a certain duration, and then the load dropped instantaneously rather than gradually. The failure state was defined as when the load decreases rapidly and the FRP loses its contribution. The load–deflection response of the tested specimens can be seen in Fig. 10. The first graph (Fig. 10a) shows the deflection at the center of the beam corresponding to the total load (R_1+R_2), while the second graph (Fig. 10b) shows the average deflection at the loading points, corresponding to the average load $(R_1+R_2)/2$ for shear span. The shear-strengthened specimens did not show a noticeable improvement in initial stiffness compared to control specimens (TC). The TC specimen reached the maximum load after passing the linear elastic range and immediately lost its strength, but on the other hand, the specimens shear-strengthened with PLNSM reinforcement showed a certain plastic deformation and then reached the maximum strength with a gradual increase in strength. The maximum strengths of the TP-3I90 and TP-3I45 specimens were found to be improved by 13.8% and 25.9%, respectively, compared to the TC specimen. And at the maximum load, the deflections at their loading points are 17.04 and 16.86 mm, respectively, which are much larger than the 6.15mm of the TC specimen. From this, it can be seen that the maximum strength and deflection at that time can be increased by using PLNSM reinforcement, and in particular, the strength can be further increased by using IPLNSM reinforcement. However, the displacements at which the TP-3I90 and TP-3I45 specimens reached their maximum load were similar. The maximum load of the T2L specimen shear-reinforced with EBR CFRP sheets also increased by 13.4% compared to the TC specimen. This is a similar value to 13.8% of TP-3I90. Nevertheless, the deflection at the maximum load was 9.83 mm, significantly lower than that observed in the TP-3I90 and TP-3I45. This is because, in the case of the NSM FRP strip, each strip effectively resisted shear cracking, while in the case of the EB FRP sheet, shear cracks in the concrete occurred at the edges of the FRP sheet, and strain was concentrated in these cracks, resulting in relatively brittle behavior.

For specimens strengthened in shear by combining the IPLNSM and EBR methods, TP-2I45-2L showed an improved maximum strength of 28.0% with deflection of 14.60 mm, which is higher than 13.4% of the T2L specimen strengthened by only EBR method. The load–deflection curves exhibited CFRP sheet debonding, characterized by a sudden drop in load after reaching the maximum value. However, in TP-2I45-2L specimen, the load was sustained at a maximum level even after debonding initiation, suggesting a delayed CFRP sheet debonding failure while also improving the deformation capacity. Therefore, shear strengthening using the hybrid method improves the strength and the load carrying capacity after the peak load was reached.

3.3 Strains of CFRP Shear Reinforcements

The strain responses of the CFRP strips for shear strengthening in TP-3I45 and TP-2I45-2L are shown in Fig. 11. The strains of the CFRP shear reinforcements of other test specimens were not measured. In TP-3I45 specimen, it was observed that the strain activity primarily occurred in the second CFRP strip (S2), where the shear crack initiated. Furthermore, the strain gradually increased up to the failure. In other words, the strain was high as a crack formed through the second NSM CFRP strip, whereas the strain was not high up to the maximum load in the other two CFRP strips as the cracks did not intersect. As the load increased, the continuous strain of the second NSM CFRP strip increased, which means that the NSM CFRP strip in the inclined direction effectively resisted the principal stress generated by the applied load. At the maximum load, the strain of the third NSM CFRP strip (S3) increased rapidly, due to the sudden increase in stress across this CFRP strip and subsequent crack formation.

In the TP-2I45-2L specimen, the first NSM CFRP strip showed the highest strain, and the strain of the CFRP sheet attached at the same location also increased. After the strain of the CFRP sheet and strip continuously increased up to 250 kN, the strain of the NSM strip decreased, indicating local bond slip. At about 380 kN, the CFRP sheet showed local debonding, and the stress was taken over from the CFRP sheet to the CFRP strip until the failure. In this specimen, the entire web part of the beam is wrapped with an CFRP sheet, so the internal cracking state cannot be observed, but it can be expected that the stress across the first NSM CFRP strip is high, and cracks have occurred in this area accordingly. Based on strain activity observed in CFRP strip and sheet, it can be deduced that the components of the hybrid approach effectively act in a composite manner to resist shear load.

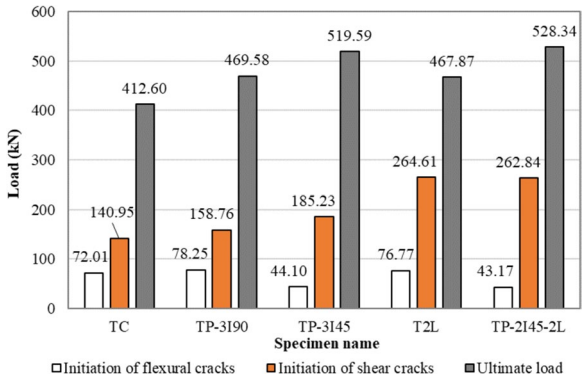

Fig. 9 Strength comparison

3.4 Strain of NSM-CFRP Reinforcement for Flexure

The strain response of CFRP strip used for flexural reinforcements is shown in Fig. 12. The strain of flexural steel reinforcement was not recorded due to errors during the test. The strain of the flexural steel reinforcement is expected to be similar to that of the nearby NSM flexural FRP. The yield strain of the tensile rebar, 2700 $\mu\varepsilon$, is added in Fig. 12. It can be seen that all specimens passed the elastic range, indicating that the specimens had yielded at around the yield strain of tensile rebar. It means that in the case without additional FRP shear reinforcements, brittle behavior due to sever shear failure, but the specimens shear reinforced with FRP reinforcement show some degree of flexural behavior even if serious shear failure occurs within the shear region.

In the TC specimen strengthened only for flexure with NSM CFRP, the strain of the CFRP was approximately 3400 $\mu\varepsilon$ until the failure. On the other hand, the T2L, TP-3I90, and TP-3I45 specimens showed strains of 5600 $\mu\varepsilon$, 5500 $\mu\varepsilon$, and 5900 $\mu\varepsilon$, respectively, which were higher compared to those of the TC specimen. The increment in strain indicated a transition from flexure-dominated behavior to shear-dominated behavior as load increased and severe shear cracking occurred. In the TP-2I45-2L specimen, which was shear-strengthened using hybrid approach combining the IPLNSM CFRP strips and EBR CFRP sheets, the flexural CFRP reinforcement exhibited a strain of 9500 μ, which is higher than that of the others, resulting in the formation of more flexural cracks, as shown in Fig. 7. Furthermore, by comparing TP-2I45-2L and TP-3I45, it was observed that their strength was nearly identical. However, the strain of the CFRP flexural reinforcement in TP-2I45-2L was significantly higher due to the advantage of employing a hybrid approach at the anchorage zone. Moreover, the strain increment was observed in all specimens until failure, indicating that the CFRP strip effectively distributed stress without experiencing any bond slip. Therefore, based on the above discussion, it can be deduced that the shear crack opening at the anchorage zone did not affect the performance of the partially debonded NSM. Additionally, by covering the anchorage zone with the hybrid approach, the strain was scientifically increased.

3.5 Theoretical Evaluation of Shear Strength

For the evaluation of shear strength of the beams, the theoretical predictions using ACI 440.2-17 (2017) and Fib-14 (2001) were performed. However, these documents

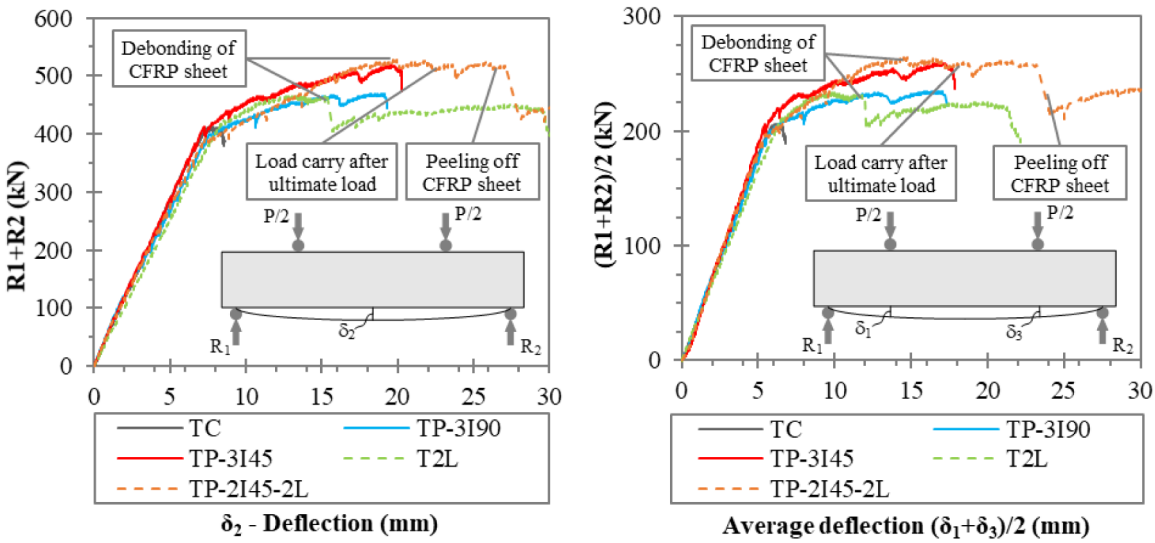

a) Load-deflection curve at center point

b) Load-deflection curve at loading point.

Fig. 10 Load–deflection curve

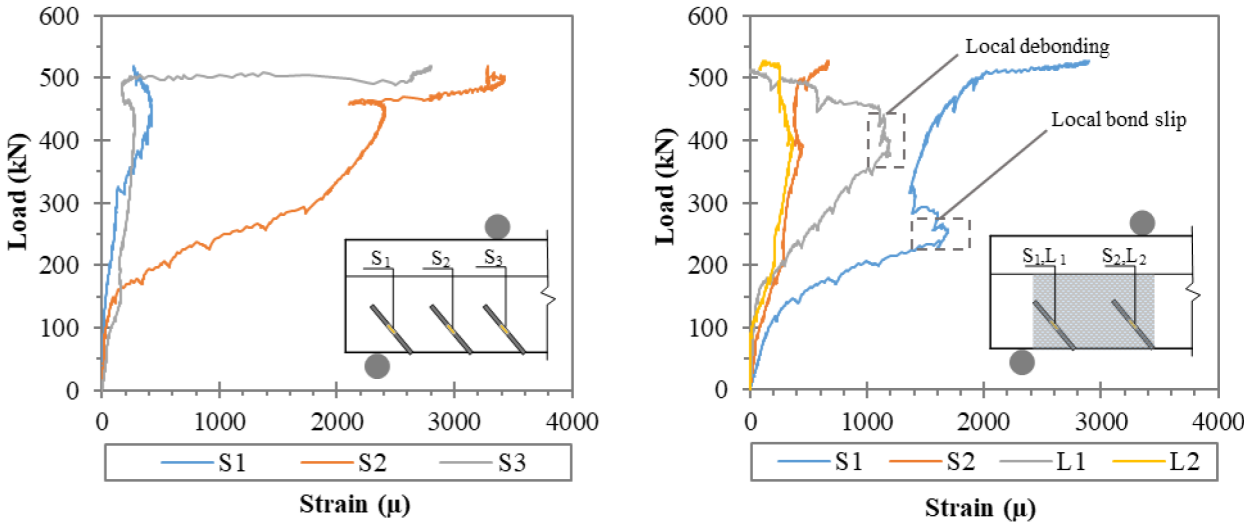

Fig. 11 Strains of CFRP reinforcements for shear

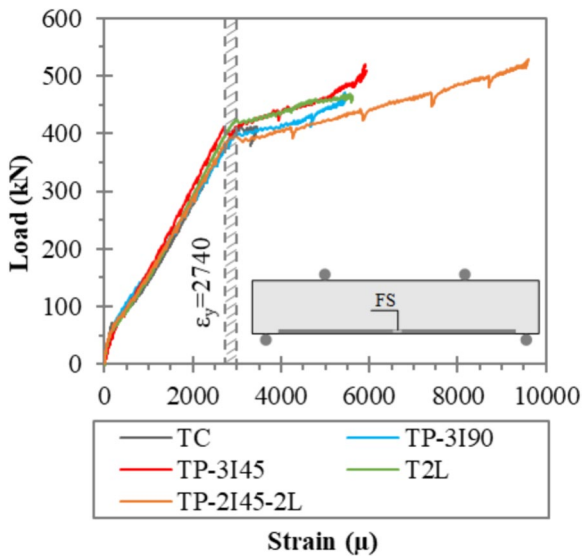

Fig. 12 Strains of CFRP reinforcements for flexure

are not serving the NSM shear strengthening. Therefore, two distinct formulations suggested by Nanni et al., (2004) and Dias and Barros (2013) were also included in doing the evaluation. Nanni's semi-empirical formulation is based on the total crack intercepting length of NSM, while Dias and Barros' curve fitting-based formulation is based on experimental results of beams shear strengthened with full-length NSM reinforcements. Therefore, the evaluation aimed to determine whether these calculation formulas could be applied effectively with a reduced NSM length.

3.5.1 Nanni et al.'s Method for NSM Strips

According to the formulation by Nanni et al., (2004), the design shear strength provided by the NSM reinforcement as shown in Fig. 13 can be determined by calculating the force resulting from the tensile stress in the CFRP strip across the assumed crack using Eq. (1):

$$V_f = 4\left(a_f + b_f\right)\tau_b L_{\text{tot}}, \tag{1}$$

where a_f and b_f are cross-sectional dimensions of the rectangular strip, τ_b is average bond stress of the CFRP elements intercepted by the shear failure crack. L_{tot} can be represented by Eq. (2):

$$L_{\text{tot}} = \sum_i L_i, \tag{2}$$

where L_i represents the length of each single CFRP strip intercepted by shear crack, expressed as:

$$\begin{cases} \min\left(\frac{s_f}{\cos\alpha + \sin\alpha}; l_{\max}\right) & i = 1 \ldots \frac{N}{2} \\ \min\left(l_{\text{net}} - \frac{s_f}{\cos\alpha + \sin\alpha} i; l_{\max}\right) & i = \frac{N}{2} + 1 \ldots N \end{cases}, \tag{3}$$

where i is the condition numbering for using Eq. (3), which is considered rounded off to the lowest integer (e.g., $i = 1.5 \Rightarrow i = 1$), α is the inclination angle of CFRP strip, s_f is the horizontal spacing of CFRP strip and l_{net} is the net length of the CFRP strip defined in Eq. (4):

$$l_{\text{net}} = l_b - \frac{2c}{\sin\alpha}, \tag{4}$$

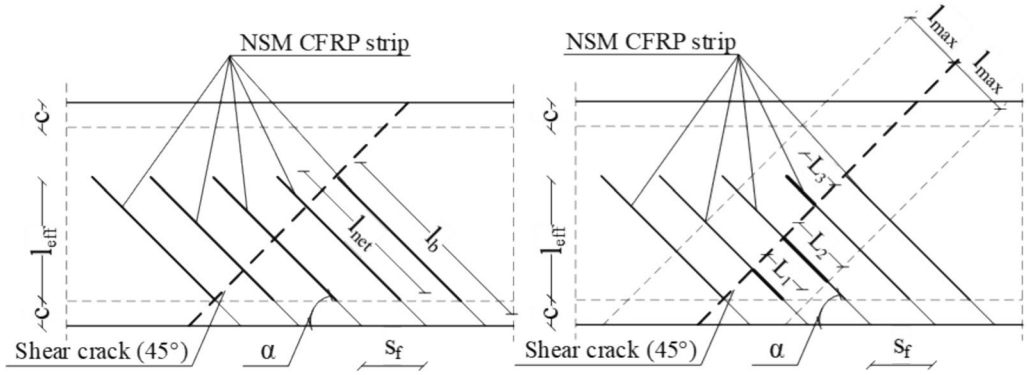

Fig. 13 Sketch showing parameters used in Nanni et al., (2004)

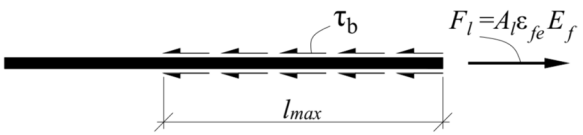

Fig. 14 Demonstration of l_{max}

where l_b is the actual length of CFRP strip and c is concrete cover.

The first limitation of Eq. (3) considers bond as the controlling failure mechanism, and represents the minimum effective length of a CFRP strip intercepted by a shear crack as a function of the term N:

$$N = \frac{l_{\text{eff}}(1 + \cot \alpha)}{s_f}, \tag{5}$$

where N is the number of strips crossed by the shear crack, which is considered rounded off to the lowest integer. (e.g., $N = 1.5 \Rightarrow N = 1$), and l_{eff} is the vertical length of l_{net} as shown in Fig. 13 and can be written as follows:

$$l_{\text{eff}} = l_b \sin \alpha - 2c. \tag{6}$$

The second limitation in Eq. (3), $L_i = l_{\max}$, results from the force equilibrium condition in Fig. 14, taking an upper bound value for the effective strain as shown in Eq. (7). For the calculation, the suggested values obtained from the pull-out test of FRP strip by Barros and Dias (2006) of $\tau_b = 16.1$ MPa and $\varepsilon_{fe} = 0.0059$ were used in this study:

$$l_{\max} = \frac{\varepsilon_{fe}}{2} \frac{a_f b_f}{a_f + b_f} \frac{E_f}{\tau_b}, \tag{7}$$

where E_f is the elastic modulus of the CFRP strip.

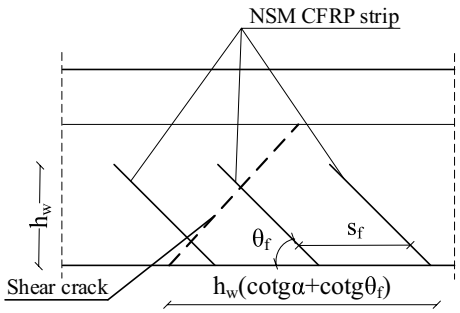

Fig. 15 Analytical formulation parameters for determining effective strain (Dias & Barros, 2013)

3.5.2 Dias and Barros's Method for NSM Strips

Dias and Barros (2013) suggested Eq. (8) to estimate the CFRP strip's contribution to the shear resistance V_f with reference to Fig. 15:

$$V_f = h_w \frac{A_{fv}}{s_f} \varepsilon_{fe} E_f \left(\cot g\alpha + \cot g\theta_f\right) \sin \theta_f, \tag{8}$$

where h_w is the height of CFRP strip; A_{fv} is the cross-sectional area of a CFRP strip; s_f is the horizontal spacing of CFRP strip; E_f (GPa) is the elastic modulus of the CFRP strip; $\alpha = 45°$ is the orientation of the shear failure crack, θ_f is the inclination of the CFPR strip.

The effective strain in the NSM strip, ε_{fe}, can be determined as:

$$\varepsilon_{fe} = C_1 \left[\frac{E_f \rho_f + E_s \rho_{sw}}{f_{cm}^{2/3}} \right]^{-C_2}, \tag{9}$$

where ρ_f and ρ_{sw}. represent the ratio of CFRP and steel stirrup and in Eq. (9) f_{cm} is in MPa, E_f and E_s are in GPa. C_1 and C_2 can be obtained using Eqs. (10) and (11), respectively:

$$C_1 = 3.76888e^{\left(-0.1160261\theta_f + 0.0010437\theta_f^2\right)}, \tag{10}$$

$$C_2 = 0.460679e^{\left(0.0351199\theta_f - 0.0003431\theta_f^2\right)}. \tag{11}$$

Because Eq. (9) does not cater to all the effects influencing the effectiveness of the CFRP strip, an uncertainty factor, designated $\gamma_f = 1.3$ can be used, as proposed by Dias & Barros, 2013. Following this criterion, Eq. (9) can be expressed by Eq. (12):

$$\varepsilon_{fe} = \frac{C_1\left[\frac{E_f\rho_f + E_s\rho_{sw}}{f_{cm}^{2/3}}\right]^{-C_2}}{\gamma_f}. \tag{12}$$

3.5.3 ACI 440 Formulation for EBR Method

According to ACI 440.2-17 2017, the contribution of CFRP to the shear resistance as in Fig. 16 is given by:

$$V_f = \psi_f \frac{A_{fv}(\sin\alpha + \cos\alpha)f_{fe}d_f}{s_f}, \tag{13}$$

where ψ_f is reduction factor for the three-sided FRP U-wrap or two-opposite-side recommend by ACI 440.2-17 2017 and 0.85 is used, d_f is the effective depth of the sheets which is depth measured from the tension reinforcement to the edge of the sheet, s_f is the spacing of the wet lay-up strips of CFRP sheets, α is the inclination angle of CFRP's fiber, A_{fv} is the area of CFRP shear reinforcement with in spacing s_f as shown in Fig. 16:

$$A_{fv} = 2nt_f w_f, \tag{14}$$

where n, t_f and w_f are the number of plies, the thickness of a layer and the width of the sheet, respectively. In the case of continuously bonded shear CFRP sheet, so s_f equal to w_f. The effective stress in the CFRP, f_{fe}, is obtained multiplying the elastic modulus of the CFRP, E_f, by the effective strain as defined by Eq. (15):

$$\varepsilon_{fe} = k_v\varepsilon_{fu} \le 0.004 \text{ (for U - wraps)}, \tag{15}$$

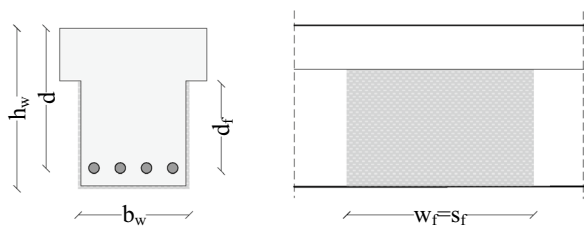

Fig. 16 Dimensional variables in using EBR method using CFRP sheet

where k_v is a bond-reduction coefficient related to the concrete strength, the type of wrapping scheme used, and the stiffness of the CFRP sheet. It can be calculated using Eq. (16):

$$k_v = \frac{k_1k_2L_e}{11900\varepsilon_{fu}} \le 0.75, \tag{16}$$

with

$$L_e = \frac{23300}{\left(nt_fE_f\right)^{0.58}}, \tag{17a}$$

$$k_1 = \left(\frac{f_c'}{27}\right)^{2/3}, \tag{17b}$$

$$k_2 = \frac{d_f - L_e}{d_f}, \tag{17c}$$

where f_c' is the 28-day concrete compressive strength, L_e is the active bond length, k_1 and k_2 are modification factors that account for the concrete strength and for the wrapping scheme used, respectively.

3.5.4 Fib-14 Formulation for EBR Method

In the Fib-14 2001, for the CFRP fiber with orthogonal to the beam axis, the contribution of the CFRP to the shear resistance of a concrete member can be written in the following form:

$$V_f = 0.9\varepsilon_{fe}E_f\rho_f b_w d_f cot(\theta), \tag{18}$$

where E_f is the elastic modulus of CFRP sheet, b_w is the width of beam's web, d_f is the effective depth of the sheets from the tension reinforcement to the edge of the sheet, θ is the angle of diagonal crack with respect to the member axis and assumed equal to 45°, ρ_f is the CFRP sheet reinforcement ratio and for continuously bonded equal to:

$$\rho_f = \frac{2nt_f}{b_w}, \tag{19}$$

where n and t_f are the number of plies and the thickness of a layer, respectively, and $\varepsilon_{fe,d}$ is the design value of effective strain in the CFRP, that can be obtained from ε_{fe}:

$$\varepsilon_{fe} = min\left[0.65\left(\frac{f_{cm}^{2/3}}{E_f\rho_f}\right)^{0.56}10^{-3}; 0.17\left(\frac{f_{cm}^{2/3}}{E_f\rho_f}\right)^{0.30}\varepsilon_{fu}\right] \tag{20}$$

(f_{cm} in MPa and E_f in GPa).

For f_{cm} is the cylinder average concrete compressive strength and ε_{fu} is the ultimate CFRP strain. Applying

safety factor provided by Fib Bulletin 14, $\varepsilon_{fe,d} = \frac{\varepsilon_{fe}}{\gamma_f}$, where γ_f is partial safety factor that depends on failure modes of CFRP sheet. $\gamma_f = 1.3$ was used for bond failure leading to peeling off dominates.

3.5.5 Comparison of Result with Theoretical Formulations

The experimental results were compared with theoretical formulations previously mentioned. The overall calculation results are shown in Table 5 with the experimental results expressed as 1/2 of the maximum load as the value for one shear span V_e. Furthermore, the shear strengths contributed by the CFRP strip and sheets were obtained by subtracting the shear strength of the TC specimen not strengthened with CFRP (control specimen) from that of each specimen strengthened with CFRP, denoted by V_{fe}. The nominal flexural strength of the specimens was calculated following the calculation process of Seo et al., (2016a, 2016b), represent by P_n. For all specimens, it can be seen that the shear strength is lower than the flexural strength, as intended in the specimen design.

In the prediction of shear strength V_{f1} using Nanni et al., (2004), the shear force resisted by the CFRP strip is significantly influenced by the effective length of the CFRP strips crossing crack. The calculation results indicate that there is no contribution of NSM CFRP for shear in TP-3I90 specimen because none of CFRP strip cross crack in Eq. (5). In the crack pattern of the specimen as shown in Fig. 8b, a clear crack penetrating the actual CFRP reinforcement is not visible. However, it can be seen that the angle of the cracks with respect to the horizontal axis of the beam increased between two strips and shear cracks occurred more than TC specimen. This means that although there is a shear reinforcement effect of NSM-CFRP of reduced length, this is not properly reflected in the Nanni's calculation process. However, in cases where an effective length is provided, such as in the TP-3I45 specimen, the shear estimation closely aligns with the experimental results by comparing V_{fe} and V_{f1}.

The formulations provided by Dias and Barros (2013) look almost similar to those of ACI 440 in evaluating the shear strength. The difference is the effective strain of CFRP that is calculated based on curve fitting of test results performed on full-length CFRP strips. Predicted values V_{f2} obtained from this equation are lower than the test results V_{fe} due to the conservative estimation of effective strain in Eq. (12).

The ACI 440 and Fib 14 formulations were used to estimate the shear capacity of the specimen strengthened using the EBR method. In the case of the T2L specimen retrofitted with the EBR method, ACI 440 predicted value V_{f3} closely aligned with the test results, suggesting a reliable estimation. However, the contribution of CFRP sheets V_{f4} was overestimated in the case of using the Fib Bulletin 14.

The capacity of the combined effect can be determined by summing the individual contributions from each component. This assumption is based on the premise that the CFRP strip and sheet work together as a composite to increase the overall capacity, as observed in Sect. 3.3. As the results, it can be found that the combination of Nanni formulation and ACI 440 showed reasonable results in estimating capacity of hybrid approach.

The total shear strength V_n is calculated by summing the shear strength provided by concrete and steel stirrup with the reliably calculated shear contribution of CFRP. Based on the above discussion, Nanni's and ACI 440 methods are selected to calculate the total shear strength. By comparing analytical and experimental results, it is shown that these methods are reliable in estimating the shear strength, and the ratio of V_e/V_n is higher than one, indicating a safe condition.

Table 5 Evaluation on the strength of RC beam strengthened with CFRP reinforcements

Specimen name	V_e	V_{fe}	P_n	NSM FRP strip		EBR FRP sheet		ACI 318 V_c	ACI 318 V_s	V_n	$\frac{V_e}{V_n}$
				Nanni V_{f1}	Dias V_{f2}	ACI 440 V_{f3}	FIB-14 V_{f4}				
	(kN)	(kN)	(kN)	(kN)	(kN)	(kN)	(kN)	(kN)	(kN)	(kN)	
TC	206.3	-	301.03	–	–	–	–	52.62	148.82	201.44	1.02
TP-3I90	234.79	28.49		0.00	6.56	–	–			201.44	1.17
TP-3I45	259.79	53.49		35.47	6.38	–	–			236.91	1.10
T2L	233.94	27.64		–	–	27.56	30.44			229.0	1.02
TP-2I45-2L	264.17	57.87		14.75	5.51	27.56	30.44			243.75	1.08

V_e is test result, V_{fe} is the contribution of CFRP to the shear resistance, P_n is the nominal flexural strength by following Seo's process [18] and $V_n = V_c + V_s + V_{f1} + V_{f3}$ is reliable prediction of shear strength

4 Conclusions

The purpose of this study was to experimentally investigate and remedy the effect of reducing the length of NSM CFRP for shear in an RC T-beam. The effect was evaluated by analyzing the beam's load capacity, stiffness, failure modes, strain of CFRP reinforcement and comparing the results to existing formulations. The study's findings are summarized as follows:

1. Providing the shear retrofit with a reduced length of NSM to 60% of the height of the beam's web did not have any negative effect on the strength; instead, it led to increased strength and improved deformation capacity. Furthermore, inclining the NSM retrofitting proved more effective in intercepting the shear cracks than the vertical placement.
2. The hybrid approach combining the IPLNSM CFRP strips and EBR CFRP sheets, is more effective than using the either method individually. The hybrid approach significantly improves the shear strength as well as deformation capacity.
3. Applying the partially debonded NSM method for flexure retrofitting, the shear crack opening at the anchorage zone did not affect its performance. Furthermore, covering the anchorage zone with the hybrid approach led to a scientifically increased strain.
4. The method proposed by Nanni et al., (2004) can also be used for designing the PLNSM reinforcement, including the configurations with inclination of the CFRP strips. However, the strengthening effect was not properly reflected in the vertically reinforced PLNSM strips.
5. The combination of Nanni's formulation for designing PLNSM reinforcement and ACI-440 for EBR strength estimation yielded reasonable agreement with the experimental findings, resulting in good prediction of the shear strength using hybrid approach.

Above results are based on limited conditions of only a few experimental results. In this regard, additional research is being prepared to quantitatively determine the change in strengthening effect as the length of the CFRP strip is reduced during vertical or diagonal shear reinforcement, and to find a design procedure that can appropriately calculate this.

Acknowledgements
The author would like to acknowledge to National Research Foundation of Korea (NRF) for the support of research fund in doing this study.

Author contributions
S. Khol: experimental work, data analysis and theoretical work, writing and reviewing the article. S.-Y. Seo: funding acquisition, project administration, conceptualizing and analyzing the study, and reviewing the article. H. V. Tran: experimental work and reviewing the article. M. U. Hanif: investigation, methodology, formal analysis, reviewing the article. All authors read and approved the final manuscript.

Funding
This research was supported by the National Research Foundation of Korea (NRF) under a grant funded by the Korean government (MSIT) (Nos. 2021R1A4A2001964, 2022R1A2C2004460).

Availability of data and materials
The experimental data will be provided on the reasonable request.

Declarations

Ethics approval and consent to participate
Not applicable.

Consent for publication
The manuscript is approved by all authors for publication. The author declares that the work described was original research that has not been published previously, and not under consideration for publication elsewhere, in whole or in part.

Competing interests
The authors declare that they have no competing interests.

Received: 24 April 2024 Accepted: 26 August 2024
Published online: 03 December 2024

References

ACI 318-19. (2019). *Building code requirements for structural concrete and commentary*. American Concrete Institute. https://doi.org/10.14359/51716937
ACI 440.2-17 (2017). *Guide for the design and construction of externally bonded FRP systems for strengthening concrete structures*. American Concrete Institute.
Al Rjoub, Y. S., Ashteyat, A. M., Obaidat, Y. T., & Bani-Youniss, S. (2019). Shear strengthening of RC beams using near-surface mounted carbon fibre-reinforced polymers. *Australian Journal of Structural Engineering, 20*(1), 54–62. https://doi.org/10.1080/13287982.2019.1565617
Al-Amery, R., & Al-Mahaidi, R. (2006). Coupled flexural–shear retrofitting of RC beams using CFRP straps. *Composite Structures, 75*(1–4), 457–464. https://doi.org/10.1016/j.compstruct.2006.04.037
Arslan, M. H., Yazman, Ş, Hamad, A. A., Aksoylu, C., Özkılıç, Y. O., & Gemi, L. (2022). Shear strengthening of reinforced concrete T-beams with anchored and non-anchored CFRP fabrics. *Structures, 39*, 527–542. https://doi.org/10.1016/j.istruc.2022.03.046
Bae, S.-W., & Belarbi, A. (2013). Behavior of various anchorage systems used for shear strengthening of concrete structures with externally bonded FRP sheets. *Journal of Bridge Engineering, 18*(9), 837–847. https://doi.org/10.1061/(ASCE)BE.1943-5592.0000420
Barris, C., Correia, L., & Sena-Cruz, J. (2018). Experimental study on the bond behaviour of a transversely compressed mechanical anchorage system for externally bonded reinforcement. *Composite Structures, 200*, 217–228. https://doi.org/10.1016/j.compstruct.2018.05.084
Barros, J. A. O., & Dias, S. J. E. (2006). Near surface mounted CFRP laminates for shear strengthening of concrete beams. *Cement and Concrete Composites, 28*(3), 276–292. https://doi.org/10.1016/j.cemconcomp.2005.11.003
Dias, S. J. E., & Barros, J. A. O. (2010). Performance of reinforced concrete T beams strengthened in shear with NSM CFRP laminates. *Engineering Structures, 32*(2), 373–384. https://doi.org/10.1016/j.engstruct.2009.10.001
Dias, S. J. E., & Barros, J. A. O. (2013). Shear strengthening of RC beams with NSM CFRP laminates: Experimental research and analytical formulation. *Composite Structures, 99*, 477–490. https://doi.org/10.1016/j.compstruct.2012.09.026
Dias, S. J. E., & Barros, J. A. O. (2017). NSM shear strengthening technique with CFRP laminates applied in high T cross section RC beams. *Composites Part*

b: Engineering, 114, 256–267. https://doi.org/10.1016/j.compositesb.2017.01.028
Dias, S. J. E., Silva, J. R. M., & Barros, J. A. O. (2021). Flexural and shear strengthening of reinforced concrete beams with a hybrid CFRP solution. *Composite Structures, 256*, 113004. https://doi.org/10.1016/j.compstruct.2020.113004
El-Maaddawy, T., & Chekfeh, Y. (2012). Retrofitting of severely shear-damaged concrete T-beams using externally bonded composites and mechanical end anchorage. *Journal of Composites for Construction, 16*(6), 693–704. https://doi.org/10.1061/(ASCE)CC.1943-5614.0000299
Fib-14. (2001). *Externally bonded FRP reinforcement for RC structures: technical report on the design and use of externally bonded fibre reinforced polymer reinforcement (FRP EBR) for reinforced concrete structures*. International Federation for Structural Concrete.
Godat, A., Hammad, F., & Chaallal, O. (2020). State-of-the-art review of anchored FRP shear-strengthened RC beams: A study of influencing factors. *Composite Structures, 254*, 112767. https://doi.org/10.1016/j.compstruct.2020.112767
Hassan, T., & Rizkalla, S. (2004). Bond mechanism of near-surface-mounted fiber-reinforced polymer bars for flexural strengthening of concrete structures. *ACI Structural Journal*. https://doi.org/10.14359/13458
Hong, K. N., Han, J. W., Seo, D. W., & Han, S. H. (2013). Flexural response of reinforced concrete members strengthened with near-surfaced-mounted CFRP strips. *International Journal of Physical Sciences*, *6*(5), 948–961. https://doi.org/10.5897/IJPS10.222
Jalali, M., Sharbatdar, M. K., Chen, J.-F., & Jandaghi Alaee, F. (2012). Shear strengthening of RC beams using innovative manually made NSM FRP bars. *Construction and Building Materials, 36*, 990–1000. https://doi.org/10.1016/j.conbuildmat.2012.06.068
Lorenzis, L., & Nanni, A. (2001). Shear strengthening of reinforced concrete beams with near-surface mounted fiber-reinforced polymer rods. *Structural Journal*, *98*(1), 60–68. https://doi.org/10.14359/10147
Mhanna, H. H., Hawileh, R. A., & Abdalla, J. A. (2021). Shear behavior of RC T-beams externally strengthened with anchored high modulus carbon fiber-reinforced polymer (CFRP) laminates. *Composite Structures, 272*, 114198. https://doi.org/10.1016/j.compstruct.2021.114198
Moradi, E., Naderpour, H., & Kheyroddin, A. (2020). An experimental approach for shear strengthening of RC beams using a proposed technique by embedded through-section FRP sheets. *Composite Structures, 238*, 111988. https://doi.org/10.1016/j.compstruct.2020.111988
Mostofinejad, D., Esfahani, M. R., & Shomali, A. (2019). Experimental and numerical study of the RC beams shear-strengthened with NSM technique. *Journal of Composite Materials, 53*(17), 2377–2389. https://doi.org/10.1177/0021998319830777
Nanni, A., Ludovico, M. D., & Parretti, R. (2004). Shear strengthening of a PC bridge girder with NSM CFRP rectangular bars. *Advances in Structural Engineering, 7*(4), 297–309. https://doi.org/10.1260/1369433041653570
Oller, E., Pujol, M., & Marí, A. (2019). Contribution of externally bonded FRP shear reinforcement to the shear strength of RC beams. *Composites Part b: Engineering, 164*, 235–248. https://doi.org/10.1016/j.compositesb.2018.11.065
Rizzo, A., & De Lorenzis, L. (2009). Behavior and capacity of RC beams strengthened in shear with NSM FRP reinforcement. *Construction and Building Materials, 23*(4), 1555–1567. https://doi.org/10.1016/j.conbuildmat.2007.08.014
Seo, S., Choi, K., Kwon, Y., & Lee, K. (2016a). Flexural strength of RC beam strengthened by partially de-bonded near surface-mounted FRP strip. *International Journal of Concrete Structures and Materials, 10*(2), 149–161. https://doi.org/10.1007/s40069-016-0133-z
Seo, S.-Y., Feo, L., & Hui, D. (2013). Bond strength of near surface-mounted FRP plate for retrofit of concrete structures. *Composite Structures, 95*, 719–727. https://doi.org/10.1016/j.compstruct.2012.08.038
Seo, S.-Y., Lee, M. S., & Feo, L. (2016b). Flexural analysis of RC beam strengthened by partially de-bonded NSM FRP strip. *Composites Part b: Engineering, 101*, 21–30. https://doi.org/10.1016/j.compositesb.2016.06.056
Sharaky, I. A., Torres, L., Comas, J., & Barris, C. (2014). Flexural response of reinforced concrete (RC) beams strengthened with near surface mounted (NSM) fibre reinforced polymer (FRP) bars. *Composite Structures, 109*, 8–22. https://doi.org/10.1016/j.compstruct.2013.10.051
Tanarslan, H. M., Yalçınkaya, Ç., Alver, N., & Karademir, C. (2021). Shear strengthening of RC beams with externally bonded UHPFRC laminates. *Composite Structures, 262*, 113611. https://doi.org/10.1016/j.compstruct.2021.113611

Publisher's Note

Springer Nature remains neutral with regard to jurisdictional claims in published maps and institutional affiliations.

Senghong Khol from Department of Architectural Engineering, Korea National University of Tranportation, 50 Daehakro, Chungju-Si, 27469, South Korea.

Soo-Yeon Seo from Department of Architectural Engineering, Korea National University of Tranportation, 50 Daehakro, Chungju-Si, 27469, South Korea.

Hai Van Tran from Department of Architectural Engineering, Korea National University of Tranportation, 50 Daehakro, Chungju-Si, 27469, South Korea.

Muhammad Usman Hanif from School of Civil and Environmental Engineering (SCEE), National University of Sciences and Technology, H-12 Islamabad, Pakistan.